Available online at www.sciencedirect.com
SCIENCE DIRECT®
Journal of Magnetic Resonance 165 (2003) 49–58
JMR Journal of Magnetic Resonance
www.elsevier.com/locate/jmr

Application of the NMR-MOUSE to food emulsions

H.T. Pedersen,[a,*] S. Ablett,[b] D.R. Martin,[b] M.J.D. Mallett,[c,1] and S.B. Engelsen[a]

[a] *Centre for Advanced Food Studies, Department of Dairy and Food Science, Food, Technology, The Royal Veterinary and Agricultural University, 1958, Frederiksberg C, Denmark*
[b] *Unilever R &D Colworth, Colworth House, Sharnbrook, Bedford, MK44 1LQ, UK*
[c] *University of Kent, Canterbury, Kent CT2 7NR, UK*

Received 21 April 2003; revised 17 June 2003

Abstract

The application of the NMR-MObile Universal Surface Explorer (NMR-MOUSE) to study food systems is evaluated using oil-in-water emulsions, and the results are compared to those obtained using a conventional low-field NMR (LF-NMR) instrument. The NMR-MOUSE is a small and portable LF-NMR system with a one-sided magnet layout that is used to replace the conventional magnet and probe on a LF-NMR instrument. The high magnetic field gradients associated with the one-sided MOUSE magnet result in NMR signal decays being dominated by molecular diffusion effects, which makes it possible to discriminate between the NMR signals from oil and water. Different data acquisition parameters as well as different approaches to the analysis of the NMR data from a range of oil-in-water emulsions are evaluated, and it is demonstrated how the concentration of oil and water can be determined from the NMR-MOUSE signals. From these model systems it is concluded that the NMR-MOUSE has good potential for the quantitative analysis of intact food products.

Keywords: NMR; Low-field; Mouse; Water; Oil; Emulsion

1. Introduction

Low-field ^{1}H nuclear magnetic resonance (LF-NMR) is a technique that is widely used throughout the food industry, where its major application is the determination of the solid/liquid ratio of fat blends [1–5]. It is a versatile technique that is also used throughout the industry to provide information on the state and dynamics of the various components present in food such as total amount of water [6,7], total amount of fat [8,9], distribution of the water [10,11], diffusion rates of water and other small molecules [12–14], as well as what can generally be described as 'food quality parameters' (e.g., quality of meat [15–18], staling of bread [19,20] and sensory properties of cooked potatoes [21]). One of the more recent developments has been low-field nuclear magnetic resonance imaging (LF-MRI), which has potential as a tool for studying a variety of problems in the food science area [22–26]. There have also been improvements in the design of the permanent magnet, allowing water and fat in meat to be discriminated in terms of their chemical shift differences [27]. Despite the potential for rapid, non-destructive at-line/on-line process control [28–30], LF-NMR still suffers from a number of drawbacks. These are nearly all related to the designs of the probe and permanent magnet normally associated with this type of instrumentation. The instruments require a homogeneous magnetic field which in turn depends on a stable ambient temperature for the magnet, absence of vibrations and shielding from disturbing extraneous magnetic fields. In addition, the instruments cannot really be considered portable due to the size and weight (50–100 kg) of the permanent magnets. Moreover, to optimise sensitivity, they tend to be small-bore instruments, typically ranging in sample tube diameter from 10 to 30 mm, although instruments with

* Corresponding author. Present address: Applied Trinomics, Novo Nordisk, Novo Nordisk Park, 2760 Maaloev, Denmark. Fax: +45-44-44-88-88.
E-mail address: htop@novonordisk.com (H.T. Pedersen).
[1] Present address: Oxford Magnet Technology, Wharf Road, Eynsham, Witney, Oxfordshire, OX29 4BP, UK.

1090-7807/$ - see front matter © 2003 Elsevier Inc. All rights reserved.
doi:10.1016/S1090-7807(03)00243-X

larger probe diameter have been developed [31]. For this reason it is necessary in many cases to sub-sample the food to allow analysis, and therefore it cannot in the strictest sense be claimed to be a non-destructive technique. The NMR-MObile Universal Surface Explorer (NMR-MOUSE) is a small LF-NMR device that has the potential to overcome many of these limitations.

The concept of the NMR-MOUSE was first proposed in 1996 by Eidmann et al. [32] and is further described by Blümich et al. [33] and Balibanu et al. [34]. The NMR-MOUSE is a small and portable LF-NMR system with a one-sided magnet layout that replaces the conventional magnet and probe on a LF-NMR instrument (see Fig. 1 for a schematic of the NMR-MOUSE). The one-sided design of this small magnet allows unrestricted access of large intact samples, giving few restrictions to sample geometry. However, a major difference associated with this system compared to conventional LF-NMR is the greatly reduced magnetic field homogeneity. Since the magnetic field strength rapidly decreases as a function of the distance from the surface of the NMR-MOUSE, measurements are only possible close to the surface of the sample. The relatively strong magnetic field gradient (in the order of 10 T/m at the surface of the NMR-MOUSE) reduces the NMR sensitive sample volume into a thin section through the sample, rather than the total volume of sample as is normally measured by bench-top LF-NMR systems. The design of the MOUSE therefore gives a significant reduction in the signal to noise ratio when compared to bench-top LF-NMR. Furthermore, the presence of a strong magnetic field gradient can have an overriding effect on many conventional NMR experiments. This is primarily due to artefacts being introduced as a result of molecular diffusion within the high magnetic field gradients, and these are most pronounced for small molecules that can diffuse more rapidly. Most reported experiments performed so far using the NMR-MOUSE have focussed on polymer materials such as rubber [35,36], measuring properties such as weathering [37] and cross-link density [38], but a study of the influence of anisotropy on the NMR signal in tendon [39] has also been performed. In a more general paper by Guthausen et al. [40] the application of the NMR-MOUSE to soft-matter is discussed. The aim of the present study is to evaluate the potential of the NMR-MOUSE when applied to food systems. The performance of the NMR-MOUSE is compared with a standard bench-top LF-NMR system in an application in which the oil/water concentrations in a set of model emulsions are determined.

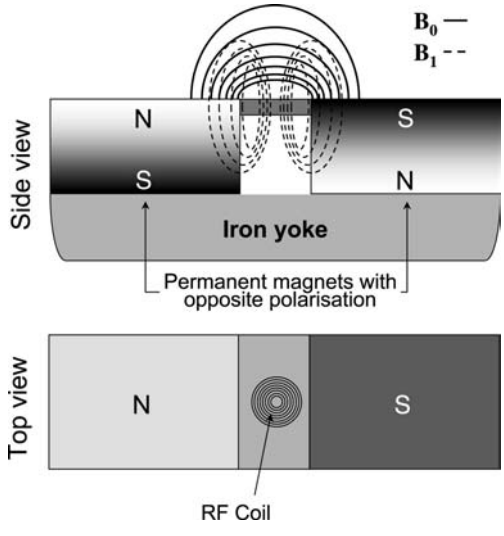

Fig. 1. Schematic drawing of the NMR-MObile Universal Surface Explorer (NMR-MOUSE).

2. Results and discussion

A schematic drawing of the MOUSE is shown in Fig. 1 and includes an approximation of the contour lines of the magnetic flux. The figure illustrates the high magnetic field gradient that is non-uniformly distributed away from the surface of the magnet. Hence, optimisation of the NMR parameters for use with this system had to be initially established.

2.1. Optimisation of the MOUSE RF frequency

The magnetic field (B_0) decreases non-linearly away from the surface of the magnet, resulting in a very high non-uniform magnetic field gradient. At a given excitation frequency, ω_0, the resulting NMR signal is received from only a thin non-uniform saddle-shaped section [34] within the sample close to the surface of the magnet, which fulfils the Larmor equation $\omega_0 = \gamma \cdot B_0$. By decreasing the resonance frequency (ω_0), the distance from the RF coil to the on-resonance region can be increased. However, the sensitivity of the RF coil is significantly reduced as a function of distance perpendicularly away from its surface. Maximum signal intensity is obtained when the thin saddle-shaped resonance condition is positioned close to the surface of the RF coil.

Fig. 2 show the amplitude of a series of signal acquisitions at different resonance frequencies performed using the rubber sample. The signal intensity has a maximum at a resonance frequency in the region of 20.8–21.3 MHz and, accordingly, a frequency of 21.0 MHz was used throughout the remainder of this study. It is interesting to note that the NMR-MOUSE produced an appreciable signal even when the resonance frequency was higher than 21.3 MHz, which is a result of the non-planar geometry of the thin resonance section. In the case of a planar resonance section an abrupt attenuation of the signal would be expected at higher

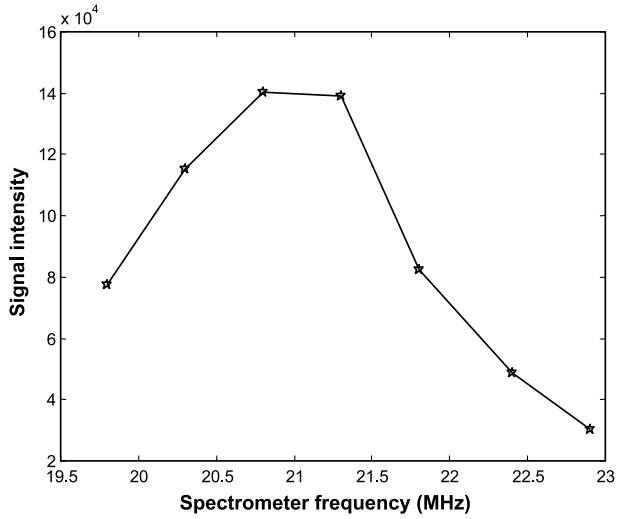

Fig. 2. NMR signal intensity measured using the NMR-MOUSE for a rubber sample as a function of the NMR spectrometer frequency.

frequencies, when the resonance condition is fulfilled below the surface of the magnet.

The shape of the sensitive volume of the NMR-MOUSE is dependent upon the shape of the RF coil and the resonance frequency used. For simplicity we usually approximate it by a small disc shaped volume. Since we are only measuring in a small volume close to the surface of the sample, the size of the sample is essentially irrelevant if the sample is homogeneous. If however it is a composite sample, only being able to measure close to the surface of the sample becomes more of a problem and reliable measurements depend on proper sub-sampling or, e.g., averaging over repeated measurements on different parts of the sample. In all situations it is only the region of the sample close to the surface that contributes to the acquired signal.

In an attempt to build a 1D-imaging MOUSE a "sweep-MOUSE" has been constructed [M.C.A. Brown et al., Surface Normal Imaging with a Single Sided NMR Device, in prep.] that allows measurement from 0 to more than 6 mm depth at a constant RF frequency by varying the magnetic field strength. The depth penetration can be further increased by decreasing the RF frequency however at the cost of signal intensity as stated in Fig. 2.

The single-sided design and small size of the NMR-MOUSE allows virtually any sample geometry to be investigated with the exception of samples with a highly convex surface shape.

2.2. Optimisation of CPMG pulse parameters

The application of a RF pulse generates a second magnetic field, B_1, which perturbs the magnetisation, M_0, away from the static magnetic field B_0. In a conventional NMR spectrometer the appropriate combination of pulse length and transmitter power rotates the magnetisation through any given angle (e.g., 90°). The length of the pulse is inversely related to the excitation bandwidth, which in the case of the NMR-MOUSE can be related to the thickness of the thin resonance slice through the sample. The RF transmitter coil on the NMR-MOUSE also generates a non-uniform B_1 field across the region of interest within the sample, which combined with the high magnetic field gradient results in a spatially varying magnetisation flip angle. It is difficult to predict what the optimum combination of pulse power and pulse length for maximum signal sensitivity should be, since simple NMR theory does not apply to the MOUSE design. The CPMG pulse sequence is normally used for spin–spin relaxation time measurements using a 90° pulse for the initial excitation followed by a sequence of 180° pulses to generate the spin echoes. In the case of the NMR-MOUSE it is not possible to set up pulses with these precise flip angles. Moreover, it is not clear if the actual flip angle for the echo train pulses in this type of CPMG experiment on the NMR-MOUSE need to be double that of the initial excitation pulse for maximum signal intensity.

The optimum parameters for use with the NMR-MOUSE were determined by systematically varying the pulse width (α), pulse power and combination of the pulse widths used in the CPMG-like pulse sequence, i.e., spin echo refocusing pulses that are either the same (i.e., pulse sequence is α–$(\tau$–α–$\tau)_n$) or twice as long (i.e., pulse sequence is α–$(\tau$–$2\cdot\alpha$–$\tau)_n$) as the initial excitation pulse. This was carried out for an oil sample, a water sample, and a 48% oil-in-water emulsion sample.

Albeit the resulting two-dimensional response surface plots proved to be sample dependent, comparison of all the signal intensities showed that an optimum signal was obtained using the α–$(\tau$–α–$\tau)_n$ pulse sequence with an α pulse width of 2 μs and a transmitter power of 300 W. This result is in agreement with previous experimental results acquired at the University of Kent at Canterbury [M.J.D. Mallett, unpublished data].

2.3. Effect of the high magnetic field gradient on the NMR signal

The high magnetic field gradient associated with the NMR-MOUSE magnet has a particularly strong influence on the relaxation properties of water and any other fast diffusing molecules present in the sample. Carr and Purcell [41] have shown that the amplitude (M_t) of a spin echo in a $\pi/2$–τ–π pulse sequence is related to the spin–spin relaxation time (T_2) and the rate of molecular diffusion (D) in a magnetic field gradient as follows:

$$M_t(\text{echo at } 2\cdot\tau) \propto \exp\left(-\frac{2\cdot\tau}{T_2} - \frac{2\cdot\gamma^2\cdot G^2\cdot D\cdot\tau^3}{3}\right), \quad (1)$$

where γ is the gyromagnetic ratio and G is the magnetic field gradient.

They also demonstrated how it is possible to dramatically reduce the effect of molecular diffusion on the NMR signal acquired in the magnetic field gradient by generating a series of spin echoes with small values of τ. This experiment is commonly referred to as the Carr–Purcell pulse sequence, where the amplitude of the nth echo at time t is expressed by

$$M_t(\text{echo at } t) \propto \exp\left(-\frac{t}{T_2} - \frac{\gamma^2 \cdot G^2 \cdot D \cdot \tau^2 \cdot t}{3}\right). \qquad (2)$$

For most conventional NMR magnets, the field inhomogeneity is sufficiently small that small τ values make the second term in Eq. (2) become negligible, even for rapidly diffusing species such as water ($D \sim 10^{-9}\,\mathrm{m^2/s}$). In these cases the T_2 relaxation rate can be readily determined directly from the observed decay. However, in the case of the NMR-MOUSE the magnetic field gradient is so large that the second term in Eq. (2) rarely can be neglected. In fact for samples with high water content, diffusion becomes the dominant factor in the observed decay rate of the signal. This is the main reason why rubber (where there is minimal molecular diffusion and quite rapid T_1 and T_2 relaxation) is a suitable reference sample for setting up experimental parameters.

The effect of applying a strong magnetic field gradient on the acquisition of CPMG decays of both water and oil was initially investigated using the bench-top LF-NMR instrument. The relaxation decay following a standard CPMG pulse is shown in Fig. 3a. The figure shows that the relaxation time of pure water is considerably longer than that of pure oil, which means the relaxation behaviour of both components are very different. When a magnetic field gradient is applied during the data acquisition, the apparent relaxation time (T_2^*) of the water decreases dramatically, whereas the oil signal is only marginally affected (see Fig. 3b). The diffusion effect is now so dominant that the apparent relaxation time of water at the applied gradient strength is reduced from being much longer to being slightly shorter than that of oil. In fact, the decay rates of the two NMR signals have become so similar that it would be difficult, if not impossible, to deconvolute them in a mixed sample.

The corresponding relaxation decay curves for oil and water using the CPMG-like pulse sequence on the NMR-MOUSE are shown in Fig. 4. From the figure it is clear that the higher magnetic field gradients on the NMR-MOUSE have strongly modified the relaxation behaviour of both components, even though the rate of diffusion of the oil is known to be relatively slow ($D \sim 10^{-12}\,\mathrm{m^2/s}$). The apparent relaxation time of water ($T_2^* = 4\,\mathrm{ms}$) is now much shorter than that of oil ($T_2^* = 94\,\mathrm{ms}$), which makes it possible to distinguish the NMR signal of water from oil.

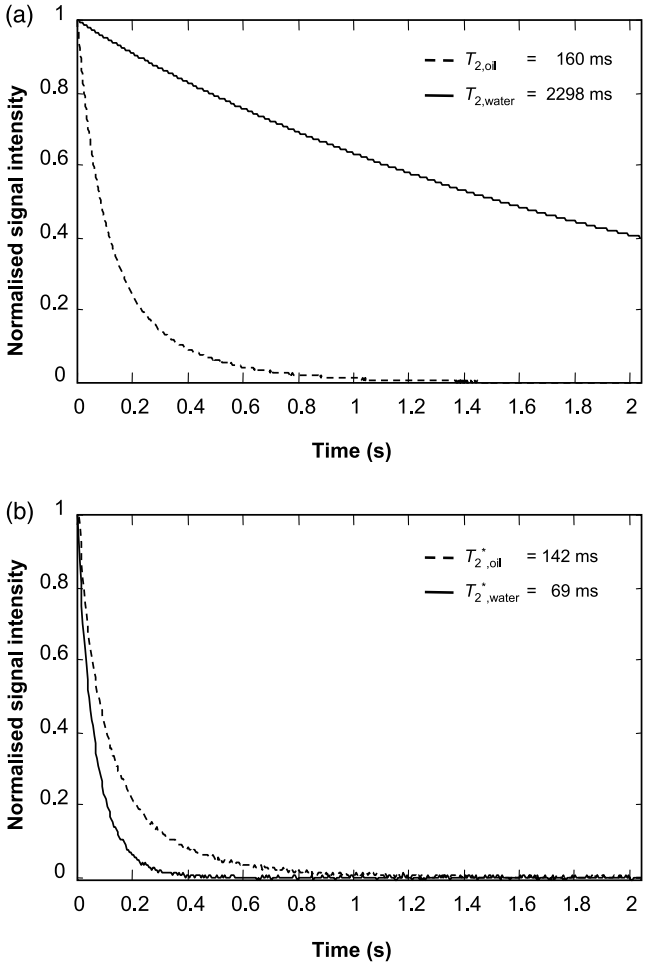

Fig. 3. NMR decay signal for pure sunflower oil and water measured using the standard CPMG pulse sequence on the bench-top LF-NMR instrument (a), together with the corresponding signal when a magnetic field gradient is applied during the signal acquisition (b).

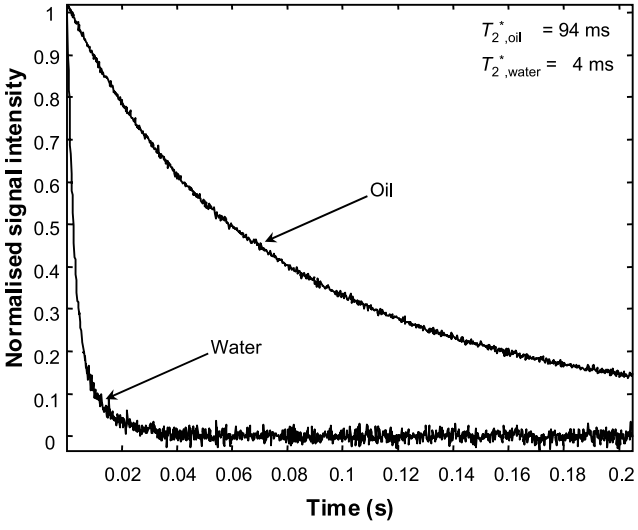

Fig. 4. NMR decay signals for pure sunflower oil and water measured using the CPMG-like pulse sequence on the NMR-MOUSE.

2.4. Comparison of the performance of NMR-MOUSE with conventional LF-NMR

Conventional LF-NMR is an efficient technique to quantitatively measure the oil and water contents of food emulsions [42–45]. For this reason we chose to compare the performance of the NMR-MOUSE to that of bench-top LF-NMR for this application. CPMG relaxation decays resulting from measuring the oil-in-water emulsions containing 10 and 67% oil recorded on the bench-top LF-NMR instrument are shown in Fig. 5a. The higher water containing emulsion can be seen to decay more slowly than the higher oil containing emulsion. The corresponding decay curves measured using the CPMG-like pulse sequence on the NMR-MOUSE is shown in Fig. 5b. Comparison of Figs. 5a and b reveals two main features:

(1) The signal/noise (S/N) ratio is approximately 10 times lower for the NMR-MOUSE than for the bench-top LF-NMR.
(2) The trend in relaxation behaviour with increasing oil content measured using the NMR-MOUSE is the reverse of that obtained using bench-top LF-NMR, which is in good agreement with the observations made in Figs. 3 and 4.

The large reduction in the S/N ratio is primarily due to the signal only being acquired from a thin slice through the sample, whereas it originates from a larger sample volume when bench-top LF-NMR is used. The reversing of the trend in the decay rates with decreasing oil contents is also expected as a result of the strong magnetic field gradient which greatly decreases the apparent relaxation time of the water due to its rapid diffusion rate.

The relative amplitude of the oil component as well as time constants resulting from the bi-exponential fitting of the decay curves from the two complete data sets acquired are shown in Table 1. This table reveals two important points. Firstly, the NMR signals obtained using both the NMR-MOUSE and bench-top LF-NMR can be readily resolved into two exponential components over the entire range of emulsions studied. Secondly, it demonstrates that both of these instrumental provide quantitative information through the relatively good agreement between the NMR-calculated and the actual concentration values. However, this agreement

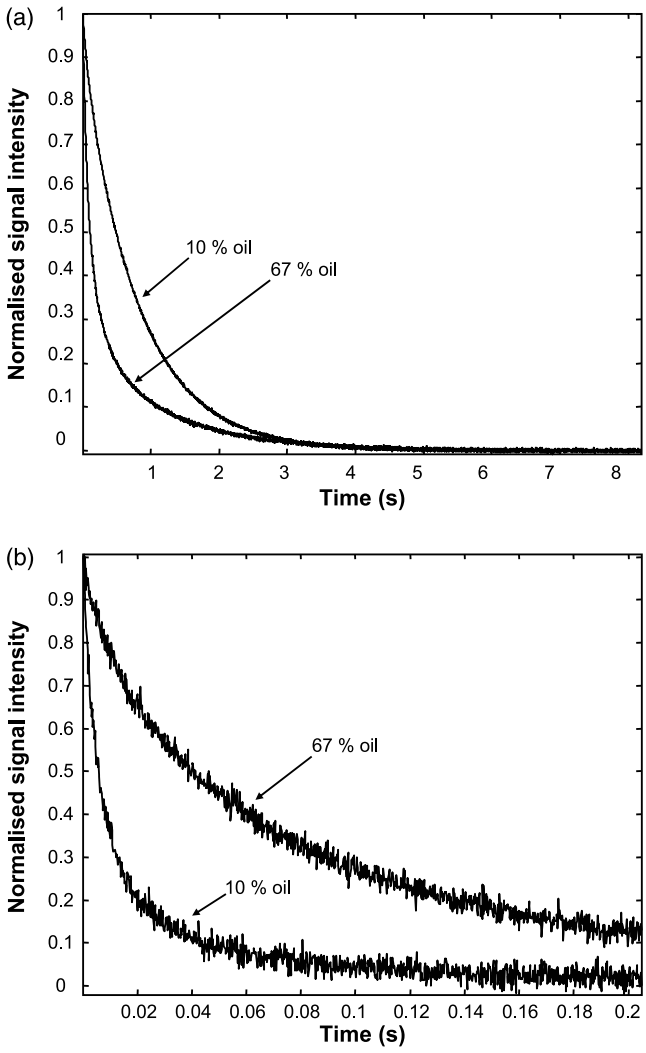

Fig. 5. NMR decay signals for the oil-in-water emulsions measured using (a) the CPMG pulse sequence on the bench-top LF-NMR instrument showing how the decay rate increases with increasing oil content and (b) the CPMG-like pulse sequence with the NMR-MOUSE showing how the decay rate decreases with increasing oil content.

Table 1
Comparison of the actual oil content of the emulsions with the calculated values based on bi-exponential fitting of the data sets acquired using the NMR-MOUSE and the bench-top LF-NMR instrument

Actual oil content (%)	MOUSE			LF-NMR		
	% Oil calculated	Water T_2^* (ms)	Oil T_2^* (ms)	% Oil calculated	Oil T_2 (ms)	Water T_2 (ms)
10	19	7	72	9	97	823
19	27	9	97	18	103	1060
29	34	9	97	27	106	1233
38	44	10	109	37	110	1477
48	52	12	113	47	112	1452
58	57	15	115	56	110	1332
67	62	20	122	65	105	1014

appears to become less precise for the emulsions with lower oil content when the NMR-MOUSE is used. It is also interesting to note that the relaxation times of the oil component in the emulsions is roughly the same on both the LF-NMR and the NMR-MOUSE, whereas the previous section showed that the relaxation behaviour of pure oil was modified by the high field gradients on the NMR-MOUSE. This is because the oil phase in the emulsions consists of small droplets within the continuous water phase, causing restricted diffusion of the oil. This therefore reduces the effects of the large field gradient on the NMR-MOUSE.

2.4.1. Comparison of mathematical routines used to analyse the NMR data

It is now well established that multivariate data analyses can be applied to bench-top LF-NMR data to help improve the prediction performance of regression models [18,46–48], and this is especially true when the noise level of the data is high. Two different regression approaches to generate prediction models of the oil content were evaluated:

(1) Linear Regression (LR) analysis on the amplitude values of the oil component obtained from the non-linear multivariate least squares fit of the data to a bi-exponential function (i.e., on the amplitude values listed in Table 1).
(2) Partial Least Squares Regression (PLSR) analysis on the entire relaxation decay curves.

The quality of the calculated prediction models using these methods on both the bench-top LF-NMR and the NMR-MOUSE data sets is reflected in the r and RMSECV values listed in Table 2. In both cases the actual oil contents, ranging from 10 to 67%, were used as reference. From Table 2 it can be seen that similar LR correlations (r) on exponential fit amplitudes are obtained for the two different data sets, but when the prediction error (RMSECV) is examined, it becomes evident that the model based on data from the bench-top LF-NMR instrument is significantly better than the model based on NMR-MOUSE data.

No meaningful PLSR model could be established for the normal bench-top LF-NMR data. This is due to large variation in the T_2 values of the water component, which were not found to vary systematically with concentration (see Table 1) preventing a simple bi-linear model. For the NMR-MOUSE on the other hand, this variation observed in T_2-values are now largely negated since the relaxation behaviour is dominated by the effects of diffusion. This means quantitative PLSR modelling is possible. When comparing the PLSR model with the LR model, it can be seen that although the two different models show a similar correlation (r) value, the prediction error (RMSECV) of the PLSR model is significantly lower which highlights the advantages of this chemometrics approach.

For all quantitative models a significant improvement in correlation and prediction error was observed when the relaxation decays were 1-normalised. In Fig. 6 the calculated oil contents are plotted for the NMR-MOUSE data using (a) values estimated by LR and (b) values estimated by the PLSR model. The centre line represents the target

Table 2
Calculated prediction models using linear regression (LR) on the amplitude of the oil component listed in Table 1 as well as the partial least squares regression (PLSR) on the entire relaxation data sets

	MOUSE		LF-NMR	
	r	RMSECV	r	RMSECV
LR	0.99	2.62	1.00	0.55
PLSR	0.99	1.81	—	—

The PLSR model is based on one component only. r is the correlation and RMSECV is the root mean square error of cross validation.

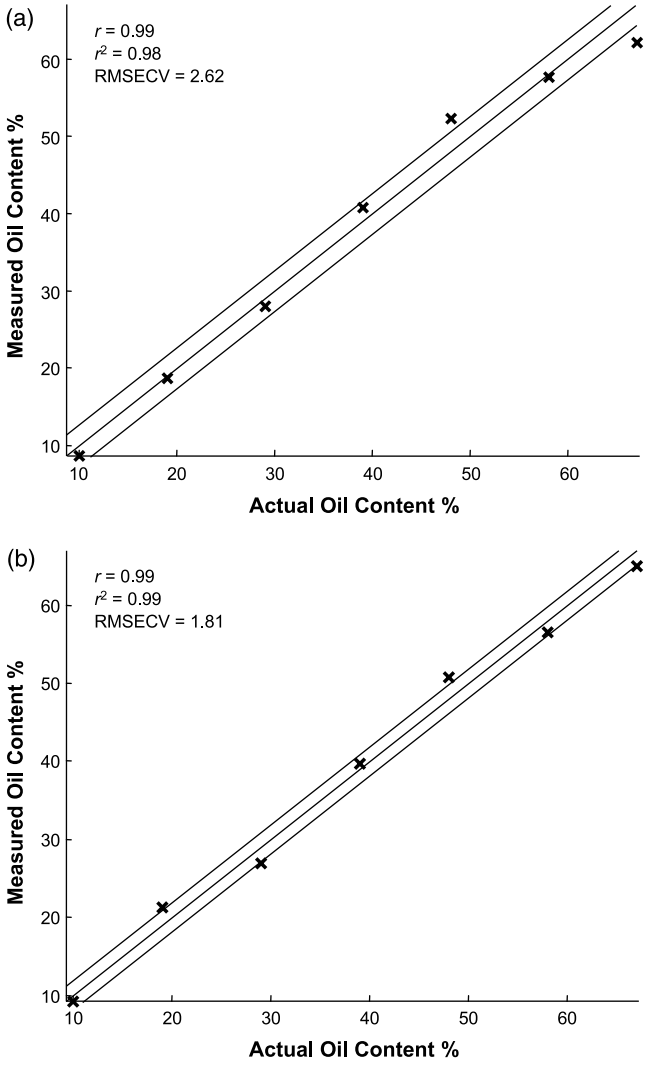

Fig. 6. Measured versus actual oil content plot for the two models calculated on the normalised NMR-MOUSE data set: (a) linear regression model based on the amplitude of the oil component of the bi-exponential fit (b) the PLSR model.

line and the two lines on either side are the ± RMSECV lines. The prediction error (RMSECV) of the LR model can be seen to be larger than with the PLRS model.

3. Conclusion

This study has demonstrated how a CPMG-like pulse sequence can be used on the NMR-MOUSE to obtain quantitative measurements on model food systems. The high magnetic field gradients associated with the one-sided NMR-MOUSE magnet result in these NMR signals being dominated by molecular diffusion effects, which make it possible to discriminate between the NMR signals from oil and water. Two different regression approaches to the analysis of the NMR data have been evaluated. When linear regressions are performed on the oil concentration extracted from bi-exponentially fitted data, the result from a traditional bench-top LF-NMR instrument displays significantly better performance than the NMR-MOUSE. When the PLSR technique is applied on the NMR-MOUSE data, this study has shown it is possible to obtain an improved quantitative performance. This indicates how it is possible to improve the quantitative determination of the oil content in oil-in-water emulsions using this chemometrics approach.

To our knowledge, this is the first reported application of the NMR-MOUSE to quantitatively study the oil and water content in an emulsion and it highlights the potential of the NMR-MOUSE technology to study intact food products near their surfaces. The obtained results are clearly encouraging for continued work with the NMR-MOUSE within the area of food analysis.

4. Experimental

4.1. Preparation of oil-in-water emulsions

Deionised water and a standard commercially available sunflower oil were used throughout this study. Triodan 55 (1%) was used as an emulsifying agent. Xanthan (1%) was added to the aqueous phase to help stabilise the emulsion and retard creaming of the oil droplets to the surface. A 67% oil-in-water emulsion was prepared using a Silverson L4R lab-scale homogeniser (Silverson Machines, Chesham, Bucks, UK). From this emulsion a series of emulsions was then prepared in the range 10–67% oil by diluting the "stock" emulsion with increasing amounts of the xanthan solution to obtain the specified concentrations.

4.2. Conventional LF-NMR measurements

Measurements were carried out using a MARAN bench-top NMR spectrometer (Resonance Instruments, Witney, UK) operating at a frequency of 11.2 MHz. The instrument is equipped with an 18 mm variable temperature field gradient probe-head, interfaced to a Crown 5000 power amplifier as the magnetic field gradient driver unit. Spin–spin relaxation decay curves were recorded by sampling the top of each echo within the Carr–Purcell–Meiboom–Gill (CPMG) pulse sequence [41,49]. A total of 8192 echoes were used, and the acquired signal was an average of 32 scans for each sample. The 90°-pulse length was 3.6 μs. Only even echoes were used in the subsequent data analysis. Other experimental conditions used for each type of samples are listed in Table 3. Varying the value of τ was found to have no significant effect on the measured spin–spin relaxation times (T_2).

Table 3
LF-NMR acquisition parameters specific to the different samples

	Oil	Water	Emulsion
90–180° pulse spacing (τ)	250 μs	1000 μs	500 μs
Recycle delay	2 s	20 s	15 s

Spin–spin relaxation decays were also recorded in the presence of a continuous magnetic field gradient. This was achieved by switching on the magnetic field gradient before the start of the CPMG pulse sequence and maintaining a constant gradient throughout the data acquisition. The following parameters were used for all samples: a total of 1024 echoes were generated with a τ spacing of 500 μs and a recycle delay of 20 s. The applied magnetic field gradient strength was 0.77 T/m, and the acquired signal was recorded as an average of 16 scans. Again only the top of each even numbered echo generated within the CPMG part of the pulse sequence was used in the subsequent data analysis. All measurements performed on the MARAN bench-top spectrometer were performed at 25 °C.

4.3. NMR-MOUSE measurements

The NMR-MOUSE was supplied by the University of Kent at Canterbury, UK, and designed to have a magnetic field strength of approximately 0.5 T (i.e., ^{1}H resonance frequency of approximately 21 MHz) at the surface of the radio frequency (RF) coil. It was interfaced directly to the MARAN NMR spectrometer electronics (to replace the conventional magnet and probe head).

Standard commercial rubber (pencil eraser) was used as a simple test material for optimising the experimental parameters used with the NMR-MOUSE. The optimum operating resonance frequency was evaluated by systematically tuning the surface coil to different frequencies in the region of 21 MHz and then acquiring the NMR signal from the rubber (at each of these frequencies).

Two different CPMG-like pulse sequences were evaluated: one similar to a standard CPMG where the flip angle of the echo pulses was twice that of the initial excitation pulse, and the other where the flip angle of the echo pulses was the same as that of the initial excitation pulse. The relationship between transmitter RF power and pulse length was evaluated in a series of experiments using water, oil and a 48% oil-in-water emulsion. In this experiment the transmitter power was systematically increased from 15 to 300 W in 15 W steps, and the pulse length was increased in steps of 0.1 μs in the range from 1.5 to 3.0 μs for oil and water samples and in the range from 1.5 to 3.5 μs for the emulsion samples. For the optimisation of these parameters the first eight echoes were acquired, each containing 64 points, and the data were recorded as an average of 32 scans. For all the subsequent measurements the acquired signal was recorded as an average of 64 scans including 1024 echoes, and rather than digitising just a single point at the top of each echo, 16 points were sampled around the centre of the echo with a dwell time of 0.5 μs. For all measurements using the NMR-MOUSE a τ spacing of 100 μs was used and recycle delays were the same as those reported in Table 3 for the bench-top LF-NMR system. The signal intensity for each echo was calculated as the average of the 5 points centred at the echo peak maximum, and all echoes except the first (i.e., both odd and even echoes) were included in the data analyses. The first echo is excluded because an increase in signal intensity is always observed from the first echo to the second. The initial RF excitation pulse does not produce a saturated nuclear spin system. This is because there are a range of flip angles experienced by the spins in the excitation volume. The first echo therefore is not the response of a completely saturated spin system but of only a part of it. Subsequent RF excitation pulses cause additional spin system saturation until an optimum condition has been created. The echo decay train is then representative of the signal decay from an optimum initial condition [50].

All measurements with the NMR-MOUSE were performed at the ambient temperature of approximately 21 °C.

5. Data analysis

All data were collected in MATLAB (MathWorks, Natic, MA, US) and phase correction was performed using Principal Phase Correction (PPC) [51]. Subsequent to PPC and prior to data analysis all data were 1-normalised, i.e., normalised such that the intensity of the first data point used for all decays is equal to 1. The performed 1-normalisation does not influence the decay rates obtained from the exponential fit, only their absolute amplitudes. This procedure mimics division by sample mass and has proven to work very well in practise.

5.1. Exponential fitting

In order to obtain the transverse relaxation times and amplitudes for oil and water in the emulsion samples, bi-exponential fitting of the data was performed. Due to the large magnetic field gradient, the relaxation time constant for the NMR-MOUSE data is expressed as T_2^*. Data were fitted according to

$$M_t = \sum_i M_{0,i} \cdot \exp\left(\frac{-t}{T_{2,i}^*}\right) + E, \tag{3}$$

where $M_{0,i}$ is the amplitude of the ith exponential component, $T_{2,i}^*$ is the characteristic relaxation time constant for the ith exponential component, and E is the residual error of the fit. The curve fitting of the relaxation data was carried out using a Simplex algorithm for the non-linear characteristic relaxation time constants, $T_{2,i}^*$, combined with a least squares fit of the linear amplitude parameters, $M_{0,i}$, inside the function evaluation call [46].

5.2. Univariate regression (or linear regression)

Linear regression was performed according the following equation

$$y = b_0 + b_1 x + e, \tag{4}$$

where y is the reference measurement or known value, x is the measured variable, b_0 and b_1 are the regression coefficients and e the residual error. In this case y corresponds to the known oil contents and x corresponds to the amplitude of the oil component resulting from the discrete bi-exponential fits.

5.3. Multivariate regression (or partial least squares regression)

Partial least squares regression (PLSR) is a multivariate regression method which allows for more variables than objects and is able to deal with the high degree of co-linearity of, for example, relaxation decay curves. PLSR performs a balanced and simultaneous decomposition of the X matrix containing the "spectra" of all objects and the y vector of reference measurements in such a way that the information in the y vector is directly used as a guide for the decomposition of X, and then performs a regression on y. The reader is referred to the literature for a thorough description of the algorithm [52,53]. In this study multivariate regression was applied to the entire relaxation decay curves.

Regressions to oil content were performed using The Unscrambler 7.6 (Camo, Trondheim, Norway) and results reported include the correlation coefficient (r) for the regression line and the root mean square error of cross validation (RMSECV), which is the error between the actual concentration and the calculated concentration. All models were cross-validated and only validated results are reported.

Acknowledgments

The authors acknowledge the help of Peter Blümler, Max Planck Institute for Polymer Research, Mainz, Germany, for his help with the construction of the NMR-MOUSE and for his many helpful discussions on this topic. The Danish Research Council (SJVF) is acknowledged for financial support which made HTP's Ph.D. and stay at Unilever possible.

References

[1] E.G. Samuelsson, J. Vikelsoe, Estimation of the amount of liquid fat in cream and butter by low resolution NMR, Milchwissenschaft 26 (1971) 621–625.
[2] J.C. Van den Enden, J.B. Rossell, L.F. Vermaas, D. Waddington, Determination of the solid fat content of hard confectionery butters, J. Am. Oil Chem. Soc. 59 (1982) 433–439.
[3] P. Lambelet, Comparison of NMR and DSC methods for determining solid content of fats. Application to cocoa butter and its admixtures with milk fat, Lebensm.-Wiss. Technol. 16 (1983) 200–202.
[4] M.C.M. Gribnau, Determination of solid/liquid ratios of fats and oils by low-resolution pulsed NMR, Trends Food Sci. Technol. 3 (1992) 186–190.
[5] V.K.S. Shukla, Solid fat content: pulsed NMR versus dilatometry, Lipid Technol. 7 (1995) 135–137.
[6] N.J. Berridge, E. Crean, P.B. Mansfield, Low resolution nuclear magnetic resonance in the determination of moisture in cheese curd, J. Dairy Res. 37 (1970) 407–416.
[7] E. Brosio, F. Conti, C. Lintas, S. Sykora, Moisture determination in starch-rich food products by pulsed magnetic resonance, J. Food Technol. 13 (1978) 107–116.
[8] D.N. Rutledge, Chemometry and time domain NMR, Analysis 25 (1997) M9–M14.
[9] D.J. Le Botlan, I. Helie, A novel approach to the analysis of fats by low resolution NMR spectroscopy: application to milk and vegetable fats, Analusis 22 (1994) 108–113.
[10] P.J. Lillford, A.H. Clark, D.V. Jones, Distribution of water in heterogeneous food and model systems, in: R.J. Rowland (Ed.), Water in Polymers, American Chemical Society, Washington, DC, 1980, pp. 177–194.
[11] P. Cornillon, L.C. Salim, Characterization of water mobility and distribution in low- and intermediate-moisture food systems, Magn. Reson. Imaging 18 (2000) 335–341.
[12] L. Coppola, R. Muzzalupo, G.A. Ranieri, Temperature dependence of water self-diffusion in the gel phase of a potassium palmitate system, J. Phys. II 6 (1996) 655–664.
[13] G. Roudaut, D. van Dusschoten, H. Van As, M.A. Hemminga, M. Le Meste, Mobility of lipids in low moisture bread as studied by NMR, J. Cereal Sci. 28 (1998) 147–155.
[14] D.R. Martin, S. Ablett, A. Darke, R.L. Sutton, M. Sahagian, Diffusion of aqueous sugar solutions as affected by locust bean gum studied by NMR, J. Food Sci. 64 (1999) 46–49.
[15] J.P. Renou, J. Kopp, Ph. Gatellier, G. Monin, G. KozakReiss, NMR relaxation of water protons in normal malignant hyperthermia-susceptible pig muscle, Meat Sci. 26 (1989) 101–114.
[16] J.P. Renou, G. Monin, P. Sellier, Nuclear magnetic resonance measurements on pork of various qualities, Meat Sci. 15 (1985) 225–233.
[17] E. Tornberg, A. Andersson, G. Von Seth, Water distribution in raw pork muscle (*M. longissimus dorsi*) of different meat qualities, 39th Int. Congr. Meat Sci. Technol. (1993).
[18] J. Brøndum, L. Munck, P. Henckel, A. Karlsson, E. Tornberg, S.B. Engelsen, Prediction of water-holding capacity and of porcine meat by comparative spectroscopy, Meat Sci. 55 (2000) 177–185.
[19] P.L. Chen, Z.Z. Long, R.R. Ruan, T.P. Labuza, Nuclear magnetic resonance studies of water mobility in bread during storage, Lebensm.-Wiss. Technol. 30 (1996) 178–183.
[20] S.B. Engelsen, M.K. Jensen, H.T. Pedersen, L. Norgaard, L. Munck, NMR-baking multivariate prediction of instrumental texture parameters in bread, J. Cereal Sci. 33 (2001) 59–69.
[21] A.K. Thybo, I.E. Bechmann, M. Martens, S.B. Engelsen, Prediction of sensory texture of cooked potatoes using uniaxial compression, near infrared spectroscopy and low field ^{1}H NMR spectroscopy, Lebensm.-Wiss. Technol. 23 (2000) 103–111.
[22] T.E. Southon, A. Mattsson, R.A. Jones, NMR imaging of roots: effects after root freezing of containerised conifer seedlings, Physiol. Plantarum 86 (1992) 329–334.
[23] H.C.W. Donker, H.v. As, H.T. Edzes, A.W.H. Jans, H. Van As, NMR imaging of white button mushroom (*Agaricus bisporus*) at various magnetic fields, Magn. Reson. Imaging 14 (1996) 1205–1215.
[24] S. Takeuchi, M. Maeda, Y. Gomi, M. Fukuoka, H. Watanabe, The change of moisture distribution in a rice grain during boiling as observed by NMR imaging, J. Food Eng. 33 (1997) 281–297.
[25] J.-M. Bonny, M. Zanca, O. Boespflug-Tanguy, V. Dedieu, S. Joandel, J.-P. Renou, Characterization in vivo of muscle fiber types by magnetic resonance imaging, Magn. Reson. Imaging 16 (1998) 167–173.
[26] T.M. Guiheneuf, P.J. Couzens, H.J. Wille, L.D. Hall, Visualization of liquid triacylglycerol migration in chocolate by magnetic resonance imaging, J. Sci. Food Agric. 73 (2000) 265–273.
[27] J.P. Renou, A. Briguet, Ph. Gatellier, J. Kopp, Technical note: determination of fat and water ratios in meat products by high resolution NMR at 19.6 MHz, Int. J. Food Sci. Technol. 22 (1987) 169–172.
[28] H.A. Slight, Continuous measuring techniques for process control, Food Manuf. 45 (1970) 61–64.
[29] R.G. Wright, R.C. Milward, B.A. Coles, Rapid protein analysis by low-resolution pulsed NMR, Food Technol. 34 (1980) 47–52.
[30] C. Tellier, C.M. Guillou, P. Grenier, D. Le Botlan, Monitoring alcoholic fermentation by low-resolution pulsed NMR, J. Agric. Food Chem. 37 (1989) 988–991.
[31] R.L. Stroshine, S.I. Cho, W.K. Wai, G.W. Krutz, I.C. Baianu, Magnetic resonance sensing of fruit firmness and ripeness, ASAE paper 92-6565 (1991) 1–13.
[32] G. Eidmann, R. Savelsberg, P. Blümler, B. Blümich, The NMR MOUSE, a mobile universal surface explorer, J. Magn. Reson. Ser. A 122 (1996) 104–109.
[33] B. Blümich, P. Blümler, G. Eidmann, A. Guthausen, R. Haken, U. Schmitz, K. Saito, G. Zimmer, The NMR-MOUSE: construction, excitation, and applications, Magn. Reson. Imaging 16 (1998) 479–484.
[34] F. Bălibanu, K. Hailu, R. Eymael, D.E. Demco, B. Blümich, Nuclear magnetic resonance in inhomogeneous magnetic fields, J. Magn. Reson. 145 (2000) 246–258.
[35] A. Guthausen, G. Zimmer, P. Blümler, B. Blümich, Analysis of polymer materials by surface NMR via the MOUSE, J. Magn. Reson. 130 (1998) 1–7.
[36] A.E. Somers, T.J. Bastow, M.I. Burgar, M. Forsyth, A.J. Hill, Quantifying rubber degradation using NMR, Polym. Degrad. Stabil. 70 (2000) 31–37.
[37] G. Zimmer, A. Guthausen, U. Schmitz, K. Saito, B. Blümich, Weathering investigation of PVC coatings on iron sheets by the NMR MOUSE, Adv. Mater. 9 (1997) 987–990.
[38] G. Zimmer, A. Guthausen, B. Blümich, Characterization of cross-link density in technical elastomers by the NMR-MOUSE, Solid State Nucl. Magn. Reson. 12 (1998) 183–190.

[39] R. Haken, B. Blümich, Anisotropy in tendon investigated in vivo by a portable NMR scanner, the NMR-MOUSE, J. Magn. Reson. 144 (2000) 195–199.
[40] G. Guthausen, A. Guthausen, F. Bălibanu, R. Eymael, K. Hailu, U. Schmitz, B. Blümich, Soft-matter analysis by the NMR-MOUSE, Macromol. Mater. Eng. 276 (2000) 25–37.
[41] H.Y. Carr, E.M. Purcell, Effects of diffusion on free precession in nuclear magnetic resonance experiments, Phys. Rev. 94 (1954) 630–638.
[42] E. Brosio, F. Conti, A. Di Nola, M. Scalzo, E. Zulli, Oil and water determination in emulsions by pulsed low-resolution NMR, J. Am. Oil Chem. Soc. 59 (1982) 59–61.
[43] N.M. Barfod, N. Krog, Destabilization and fat crystallization of whippable emulsions (toppings) studied by pulsed NMR, J. Am. Oil Chem. Soc. 64 (1987) 112–119.
[44] G.A. LaTorraca, K.J. Dunn, P.R. Webber, R.M. Carlson, Low-field NMR determinations of the properties of heavy oils and water-in-oil emulsions, Magn. Reson. Imaging 16 (1998) 659–662.
[45] D. Le Botlan, J. Wennington, J.C. Cheftel, Study of the state of water and oil in frozen emulsions using time domain NMR, J. Colloid Interf. Sci. 226 (2000) 16–21.
[46] I.E. Bechmann, H.T. Pedersen, L. Nørgaard, S.B. Engelsen, Comparative chemometric analysis of transverse low-field ^{1}H NMR relaxation data, in: P.S. Belton, B.P. Hills, G.A. Webb (Eds.), Advances in Magnetic Resonance in Food Science, The Royal Society of Chemistry, Cambridge, 1999, pp. 217–225.
[47] S.M. Jepsen, H.T. Pedersen, S.B. Engelsen, Application of chemometrics to low-field ^{1}H NMR relaxation data of intact fish flesh, J. Sci. Food Agric. 79 (1999) 1793–1802.
[48] H.T. Pedersen, H. Berg, F. Lundby, S.B. Engelsen, The multivariate advantage in fat determination in meat by bench-top NMR, Innov. Food Sci. Emerg. Technol. 2 (2001) 87–94.
[49] S. Meiboom, D. Gill, Modified spin-echo method for measuring nuclear relaxation times, Rev. Sci. Instr. 29 (1958) 688–691.
[50] P.J. McDonald, B. Newling, Stray field magnetic resonance imaging, Rep. Prog. Phys. 61 (1998) 1441–1493.
[51] H.T. Pedersen, R. Bro, S.B. Engelsen, Towards rapid and unique curve resolution of low-field NMR relaxation data: trilinear SLICING versus two-dimensional curve fitting, J. Magn. Reson. 157 (2002) 141–155.
[52] P. Geladi, B.R. Kowalski, Partial least squares regression: a tutorial, Anal. Chim. Acta 185 (1986) 1–17.
[53] H. Martens, T. Næs, Multivariate Calibration, John Wiley & Sons, Chichester, 1989.